

FIG. 5. Definition of the quantities  $a$ ,  $b$ , and  $\varphi$  which characterize elliptical phonon polarization.

Let us now turn to the determination of the polarization of a general one-phonon state  $\Phi$  given by

$$\begin{aligned} \Phi &= (a_1 b_1^\dagger + a_2 b_2^\dagger + a_3 b_3^\dagger) |0\rangle, \\ |a_1|^2 + |a_2|^2 + |a_3|^2 &= 1. \end{aligned} \quad (\text{B7})$$

The norm  $P$  of the expectation value of the vector operator  $P$  is then found to be  $(|a_1|^2 + |a_2|^2)^2$ , hence

$$P = |\langle \Phi^\dagger | \mathbf{P} | \Phi \rangle| = 1 - |a_3|^2. \quad (\text{B8})$$

The amplitude of the longitudinal component is obtained from Eqs. (B7) and (B4) as

$$|a_3|^2 = 1 - |\langle \Phi^\dagger | \mathbf{P} | \Phi \rangle| = 1 - \frac{1}{3} \langle \Phi^\dagger | \mathbf{P} \cdot \mathbf{P} | \Phi \rangle. \quad (\text{B9})$$

The amplitude of the transverse components enter into the expectation values of the Stokes' parameters through

$$\begin{aligned} P_1 &= \langle \Phi^\dagger | P_1 | \Phi \rangle = a_1^* a_1 - a_2^* a_2, \\ P_2 &= \langle \Phi^\dagger | P_2 | \Phi \rangle = a_1^* a_2 + a_2^* a_1, \\ P_3 &= \langle \Phi^\dagger | P_3 | \Phi \rangle = -i a_1^* a_2 + i a_2^* a_1. \end{aligned} \quad (\text{B10})$$

In general, the transverse component of the phonon is elliptically polarized with parameters  $\alpha$  and  $\varphi$  defined in Fig. 5. These parameters can be expressed by the expectation values of the Stokes' parameters as follows:

$$\tan 2\varphi = P_2/P_1, \quad (\text{B11})$$

$$\tan \alpha = P_3/[P + (P^2 - P_3^2)^{1/2}]. \quad (\text{B12})$$

## Exciton Complexes and Donor Sites in 33R SiC

W. J. CHOYKE, D. R. HAMILTON, AND LYLE PATRICK  
Westinghouse Research Laboratories, Pittsburgh, Pennsylvania  
(Received 29 March 1965)

Polytype 33R, which, in some respects, may be considered as part 6H, part 15R, proves to be intermediate between those polytypes in many properties, among which are the exciton energy gap (3.003 eV), absorption strength, exciton binding energies (two kinds), and nitrogen donor ionization energies (0.15 to 0.23 eV). The latter three appear to be consequences of an intermediate value of electron effective mass. Nitrogen-exciton complexes (Lampert complexes) are observed in the low-temperature photoluminescence at ten of the eleven inequivalent donor sites. In this polytype, it is possible to assign spectral lines to particular sites, which we distinguish by a simple code. Both four-particle and three-particle complexes are observed, yielding phonon energies and, in addition, exciton binding energies which may be compared with those at corresponding sites in 6H and 15R. The comparison suggests that the 15R electron effective mass is about half that of 6H. For three-particle complexes, the effective-mass approximation appears to be inadequate. Thermally excited states are observed for both kinds of complexes. 33R is a member of a special series of SiC polytypes, each of which may be characterized as part 6H, part 15R. Some properties of the luminescence of higher members of this series are predicted, and their large zones and conduction-band minima are discussed.

### I. INTRODUCTION

FOR a study of donor properties, SiC has the advantage that the same donor (e.g., nitrogen) can be studied with slight changes in neighbor arrangements (at inequivalent sites in a polytype), or with slight changes in band structure<sup>1,2</sup> (by comparing polytypes).

We are now reporting on 33R SiC, in which we have observed photoluminescence due to nitrogen-exciton

complexes (Lampert<sup>3</sup> complexes) at ten of the eleven inequivalent donor sites. Such luminescence has previously been reported for the single site<sup>4</sup> of cubic SiC, for two sites<sup>1</sup> in 4H, three sites<sup>5,6</sup> in 6H, four (of a possible five)<sup>7</sup> in 15R, and six (of a possible seven)<sup>8</sup> in 21R, a total of 26 sites in six polytypes. Within a given

<sup>1</sup> Lyle Patrick, W. J. Choyke, and D. R. Hamilton, Phys. Rev. **137**, A1515 (1965).

<sup>2</sup> Certain band properties appear to be similar in all polytypes. For example, the valence-band maximum at  $\mathbf{k}=0$  is thought to be affected very little by polytype changes, and the conduction-band maxima are thought to be always on mirror planes at the large zone boundary.

<sup>3</sup> M. A. Lampert, Phys. Rev. Letters **1**, 450 (1958).

<sup>4</sup> W. J. Choyke, D. R. Hamilton and Lyle Patrick, Phys. Rev. **133**, A1163 (1964).

<sup>5</sup> W. J. Choyke and Lyle Patrick, Phys. Rev. **127**, 1868 (1962).

<sup>6</sup> D. R. Hamilton, W. J. Choyke, and Lyle Patrick, Phys. Rev. **131**, 127 (1963).

<sup>7</sup> Lyle Patrick, D. R. Hamilton, and W. J. Choyke, Phys. Rev. **132**, 2023 (1963).

<sup>8</sup> D. R. Hamilton, Lyle Patrick, and W. J. Choyke, Phys. Rev. **138**, A1472 (1965).

polytype there is the problem of assigning an observed spectral line to a particular one of the several inequivalent sites. We believe this can now be done for 33R.

Polytype 33R may be considered to be made from approximately equal parts of 6H and 15R. The eleven sites of 33R can be tagged in a way that determines a unique correspondence between the 33R sites and those of 6H and 15R, so that the "same" site may be compared in two polytypes. This leads to an explanation of certain differences in terms of electron effective mass differences and Kohn-Luttinger interference effects.<sup>9</sup>

Polytype 33R<sup>10</sup> was discovered by Thibault,<sup>11</sup> and its atomic arrangement was established by Ramsdell,<sup>12</sup> who compared experimental intensities of x-ray reflections with those calculated for several possible sets of atomic positions. It belongs to space group *R*3m, and has a large unit cell with eleven Si and eleven C atoms (hence 66 phonon branches). The slender rhombohedral cell extends a distance of 83 Å along the trigonal axis. It is not a common polytype, and its occurrence is thought to depend on the spiral growth mechanism,<sup>13</sup> in the way suggested by Frank.<sup>14,15</sup>

The donor nitrogen substitutes for carbon. Under uv illumination, both neutral and ionized donors can capture excitons, forming both four-particle and three-particle Lampert complexes. The complexes decay with photon and phonon emission, giving rise to two kinds of spectra. The four-particle spectrum is characteristic of a loosely bound center, and the three-particle spectrum is characteristic of a tightly bound center. The spectra permit one to measure various phonon energies and binding energies, and to estimate the donor ionization energies. Comparisons with 6H and 15R spectra yield information on effective mass and site differences. A preliminary report of the luminescence has been given.<sup>16</sup>

In Sec. II, we discuss some properties of SiC polytypes, introducing the Zhdanov notation.<sup>10</sup> We define certain binding energies and the relationships between them in Sec. III. The absorption spectrum, at 4.2°K, from which we determine the exciton energy gap  $E_{Gx}$  (3.003 eV), is shown in Sec. V.

The four-particle luminescence spectrum at 6°K (④ spectrum) is given in Sec. VI, and compared with 6H

and 15R spectra in Sec. VII. A convenient code for distinguishing the neighborhoods of individual sites is then introduced (Sec. VIII). It shows how the eleven 33R sites are related to those of 6H and 15R.

The three-particle spectrum (③ spectrum) is shown in Sec. IX and compared with those of 6H and 15R in Sec. X. An examination of this spectrum at high resolution shows that pairs of 33R sites derived from a single 6H site have binding energies for excitons which differ by as little as 0.1 meV in 143 meV.

The relative electron effective masses in 33R, 6H, and 15R are discussed in Sec. XI, and the validity of the effective-mass approximation for nitrogen donors is questioned. Donor ionization energies ranging from 0.15 to 0.23 eV are obtained in Sec. XII.

Thermally excited states of the complexes are observed in the luminescence measurements at 20 and 50°K (Sec. XIII) and are interpreted by comparison with similar measurements in 6H and 15R.

Finally, 33R is considered as a member of the well-known series of polytypes [(33)<sub>n</sub>32]<sub>3</sub>. Some aspects of the luminescence of higher members of the series are predicted in Sec. XIV. The relationship between band structures of 33R and the higher polytypes is considered in Sec. XV, using a large zone to indicate how a changing zone boundary controls polytype properties, and to show how this boundary changes to coincide asymptotically with the boundary of polytype 6H.

## II. POLYTYPES

Two objectives of this paper are to show in what respects 33R SiC may be considered as made from 6H and 15R polytypes, and to draw conclusions about the band structure and about donor properties by comparing 33R binding energies with those of 6H and 15R. Such polytype comparisons require a knowledge of the stacking sequences of close-packed planes which form the various polytypes. The Ramsdell notation,<sup>17</sup> used above, does not indicate the stacking sequence, hence we introduce the Zhdanov notation,<sup>18</sup> which does.

For polytypes with short repeat sequences, the ABC notation is often used to indicate the stacking order. However, for high polytypes, a much more compact notation is obtained by noting that any ordering of the letters A, B, and C is made up of sequences which are alternately in alphabetical order (with A following C) and in reverse order. The numbers of letters in such sequences form a convenient notation.<sup>19</sup> For example, in 6H SiC, the stacking notation ABCACB is alphabetical for three terms (ABCA), then reverses for three terms (ACBA), hence 6H can be written (33). In this same way, for 15R (ABCACBCABACACB), we find the

<sup>9</sup> Lyle Patrick, Phys. Rev. **138**, A1477 (1965).

<sup>10</sup> We use the Ramsdell notation. Other designations for this polytype are Type VI (Thibault), hkkkkkkkkkk (Jagodzinski), and (3332)<sub>3</sub> (Zhdanov). A discussion of polytype notation is given by A. R. Verma in *Crystal Growth and Dislocations* (Butterworths Scientific Publications Ltd., London, 1953), Chap. 7.

<sup>11</sup> N. W. Thibault, Am. Mineralogist **29**, 249 (1944); **29**, 327 (1944).

<sup>12</sup> L. S. Ramsdell, Am. Mineralogist **30**, 519 (1945). In this paper, Ramsdell uses the old designation, Type VI.

<sup>13</sup> S. Amelinckx and G. Strumane, in *Silicon Carbide*, edited by J. R. O'Connor and J. Smiltens (Pergamon Press, Inc., New York, 1960), p. 162 (see Sec. 8).

<sup>14</sup> F. C. Frank, Phil. Mag. **42**, 1014 (1951).

<sup>15</sup> R. S. Mitchell, Z. Krist. **109**, 1 (1957).

<sup>16</sup> D. R. Hamilton, Lyle Patrick, and W. J. Choyke, Bull. Am. Phys. Soc. **9**, 542 (1964).

<sup>17</sup> L. S. Ramsdell, Am. Mineralogist **32**, 64 (1947).

<sup>18</sup> G. S. Zhdanov, Compt. Rend. Acad. Sci. U.R.S.S. **48**, 39 (1945).

<sup>19</sup> These numbers can also be obtained from the "zig-zag" arrays of atoms as viewed in (1120) planes. See Refs. 15 and 17.

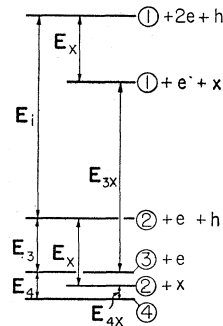


FIG. 1. Energy-level diagram. The levels represent the relative energies of various combinations of the particles which form a four-particle complex. The complex itself is the lowest level, being the most strongly bound combination. The top level represents the completely separated particles. The distances between levels give the binding energies defined in Eqs. (1) to (6).

symbol (32) repeated three times,<sup>20</sup> hence the stacking sequence for 15R is given by (32)<sub>3</sub>.

It is now clear that 33R, with symbol (3332)<sub>3</sub>, has six planes stacked like 6H, followed by five planes stacked like 15R. Of the eleven inequivalent sites in 33R, six are shown to occur in three pairs<sup>21</sup> which are very similar to the three 6H sites, the other five sites being similar to 15R sites (Sec. VIII).<sup>22</sup>

A well-known series<sup>23</sup> of SiC polytypes is constructed by adding more and more 6H groups,<sup>24</sup> as indicated in Table I. For large  $n$ , the series approaches 6H asymptotically, with the rhombohedral structures better described as faulted hexagonal.<sup>25</sup> X-ray studies<sup>26</sup> of this series show that the diffraction pattern approaches that of 6H for large  $n$ . The way in which the luminescence spectrum approaches that of 6H is already apparent in 33R, and is discussed in Sec. XIV. Similarly, the band structure of the high rhombohedral polytypes must also approach that of hexagonal 6H. The way in which this occurs can best be seen by using a *large zone* in  $\mathbf{k}$  space.<sup>27</sup> A mirror plane of the 33R large zone, shown in Sec. XV, already shows a close relationship with that of 6H.

<sup>20</sup> The threefold repetition of the sequence is characteristic of rhombohedral polytypes, hence the subscript 3 is sometimes omitted.

<sup>21</sup> In the 6H sequence (33), the two sets of three positions are equivalent under the screw displacement operation  $6_3$ . This operation is not present in rhombohedral polytypes, hence the *three* 6H sites must be put into correspondence with *six* inequivalent sites in 33R.

<sup>22</sup> Sites in different polytypes are never *identical*, but may be equivalent up to distances that are large compared with the effective Bohr radius of a donor.

<sup>23</sup> Eight polytypes in this series are known to belong to this series. See G. Singh and A. R. Verma, *Acta Cryst.* **17**, 49 (1964); Kuo Chang-lin, *Scientia Sinica* **13**, 1706 (1964).

<sup>24</sup> The polytype is thought to depend on the Burgers vector of the dislocation around which spiral growth takes place. See Ref. 15.

<sup>25</sup> One of the *high* polytypes in this series may be considered as 6H with a periodic stacking fault that becomes more and more widely spaced as  $n$  increases.

<sup>26</sup> For polytypes in this series, comparisons of x-ray reflections with those of 6H have been given by L. S. Ramsdell, Ref. 17; G. Singh and A. R. Verma, Ref. 23; and by R. S. Mitchell, *J. Chem. Phys.* **22**, 1977 (1954).

<sup>27</sup> Discussions of large zones have been given in Refs. 1 and 8. See also H. Jones, *The Theory of Brillouin Zones and Electronic States in Crystals* (North-Holland Publishing Company, Amsterdam, 1960), Chap. 5.

### III. NOTATION AND BINDING ENERGIES

We shall consider only the two Lampert complexes which result from the presence of a donor: (a) an exciton bound to a neutral donor (four-particle complex, or ④), and (b) an exciton bound to a donor ion (three-particle complex, or ③). It is convenient to use the notation of Table II to define the following six dissociation, or binding energies<sup>28</sup>:

$$\textcircled{4} \rightarrow \textcircled{3} + e - E_4, \quad (1)$$

$$\textcircled{3} \rightarrow \textcircled{2} + h - E_3, \quad (2)$$

$$\textcircled{2} \rightarrow \textcircled{1} + e - E_i, \quad (3)$$

$$x \rightarrow e + h - E_x, \quad (4)$$

$$\textcircled{4} \rightarrow \textcircled{2} + x - E_{4x}, \quad (5)$$

$$\textcircled{3} \rightarrow \textcircled{1} + x - E_{3x}. \quad (6)$$

The energies required to remove excitons from three- or four-particle complexes,  $E_{3x}$  and  $E_{4x}$ , can be expressed in terms of the independent energies defined by Eqs. (1) to (4), since the exciton may be removed one particle at a time. Thus, we obtain the following relations:

$$E_{4x} = E_4 + E_3 - E_x, \quad (7)$$

$$E_{3x} = E_3 + E_i - E_x. \quad (8)$$

We obtain the donor ionization energies by combining Eqs. (7) and (8):

$$E_i = E_{3x} - E_{4x} + E_4. \quad (9)$$

Our measurements give accurate values of  $E_{3x}$  and  $E_{4x}$ . An estimate of  $E_4$  can only be obtained rather indirectly, as outlined in Sec. VI of Ref. 6 for a 6H donor.

The relative magnitudes of the various binding energies for a nitrogen donor<sup>29</sup> in 33R SiC are thought to be as shown in Fig. 1. Each energy level in this figure represents some combination of the same four particles: (a) bound as a ④ complex in the bottom level, (b) completely separated in the top level, and (c) with various combinations of bound and unbound particles in the four intermediate levels. The six binding energies defined in Eqs. (1) to (6) are represented by the distances between levels.

TABLE I. A comparison of polytype notations.

Ramsdell notation	Zhdanov notation	No. of inequivalent C (or Si) sites
6H	(33)	3
15R	(32) <sub>3</sub>	5
33R	(3332) <sub>3</sub>	11
51R	[(33) <sub>2</sub> 32] <sub>3</sub>	17
...	...	...
(18n+15)R	[(33) <sub>n</sub> 32] <sub>3</sub>	6n+5

<sup>28</sup> These equations were given in Ref. 6.

<sup>29</sup> These levels, for a 33R donor, are discussed in Sec. XII.

TABLE II. Comparison of our notation with Lampert's. Our circled numbers are intended to suggest the number of particles in the complex.

Particle or complex	Lampert's notation	Our notation
Electron	—	$e$
Hole	+	$h$
Exciton	+—	$x$
Donor ion	⊕	①
Un-ionized donor	⊕—	②
Exciton bound to donor ion	⊕+—	③
Exciton bound to un-ionized donor	⊕+— —	④

The binding energies were originally discussed by Lampert<sup>3</sup> in terms of hydrogen analogs. We have given a diagram illustrating the relative energies, for the extreme cases of very light or very heavy holes,<sup>30</sup> and Hopfield has discussed the dependence on electron-hole mass ratios.<sup>31</sup>

#### IV. SAMPLES AND EXPERIMENTAL PROCEDURES

Our 33R samples are all from furnace runs which produced mostly 6H crystals.<sup>32</sup> The occurrence of 33R is rare and is assumed to be due to the Frank mechanism.<sup>14</sup> We can identify the observed spectra as those of the donor nitrogen, because the 33R samples are intergrown with 6H and/or 15R, whose nitrogen spectra are well known. One sample had a sufficiently large 33R portion for absorption measurements (light path 0.14 cm), and proved best for luminescence also. All measurements reported here were on this sample, but the luminescence spectra were checked by comparison with the spectra of three other 33R samples.

Our experimental procedures were the same as previously reported for similar measurements on other polytypes.<sup>5,6</sup>

#### V. ABSORPTION MEASUREMENTS

The absorption edge of 33R SiC is shown in Fig. 2. It is similar to the absorption edges of 6H and 15R and is due to indirect transitions which create excitons. We plot the square root of the absorption coefficient against photon energy, as is customary for indirect transitions.<sup>33</sup> Only the phonon *emission* part is significant at 4.2°K, and only a few of the 66 phonons give rise to resolvable structure. Polarized light was used, but only the  $E \perp C$  curve is shown. For  $E \parallel C$ , the structure is not as well resolved, and the absorption is weaker, as in other polytypes.<sup>34</sup>

<sup>30</sup> W. J. Choyke, Lyle Patrick, and D. R. Hamilton, in *Proceedings of the International Conference on the Physics of Semiconductors, Paris, 1964* (Academic Press Inc., New York, 1965), p. 751.

<sup>31</sup> J. J. Hopfield, Ref. 30, p. 725.

<sup>32</sup> D. R. Hamilton, *J. Electrochem. Soc.* **105**, 735 (1958).

<sup>33</sup> T. P. McLean, in *Progress in Semiconductors* (Heywood and Company, Ltd., London, 1960), Vol. 5, p. 55.

<sup>34</sup> Reference 5, Sec. VII.

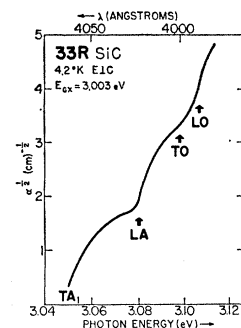


FIG. 2. Absorption edge of 33R SiC at 4.2°K, for light polarized  $E \perp c$ . The structure is characteristic of indirect exciton-creating transitions. Only the phonon-emission part is observed at this temperature, and the resolved structure is due to only a small number of the 66 phonons, as indicated.

The structure marked by letters and arrows in Fig. 2 is due to emission of some of the “principal” phonons, which have a wave vector  $\mathbf{k}$  at the *large* zone boundary, and which are very close in energy to similar phonons in other polytypes. The phonon energies are obtained much more accurately from luminescence measurements (Sec. VI), and it is the combined information from absorption and luminescence,<sup>35</sup> which gives us the value 3.003 eV for the exciton energy gap ( $E_{Gx}$ ).<sup>36</sup>

In Ref. 7, 6H and 15R absorption edges were superposed (approximately) by making a 37-meV shift of the 6H energy scale and by dividing the 6H absorption coefficients by 2.9. In the same way, the 33R edge can be approximately superposed on those of 6H and 15R. It is the similarity in electron-phonon interactions (or hole-phonon interactions) which makes this possible. Thus, the chief polytype differences are those shown in Table III, i.e., differences in energy gaps and in absorption strengths. In both respects, 33R is intermediate between 6H and 15R.

The values of  $\alpha$  in Table III are for the relatively flat portions, just before the beginning of absorption in which a longitudinal acoustical (LA) phonon is emitted. Since the absorption edges can only *approximately* be superposed, a comparison at a different part of the edge would give somewhat different ratios of absorption coefficients. However, the 33R absorption strength is everywhere intermediate between those of 6H and 15R.

It was suggested earlier that SiC valence band maxima for different polytypes are very similar, being at  $\mathbf{k}=0$ , but that many observed polytype differences

TABLE III. Exciton energy gaps at 4.2°K for three polytypes, and absorption coefficients at comparable positions on their absorption edges.

Polytype	$E_{Gx}$ (eV)	$\alpha$ ( $\text{cm}^{-1}$ )
6H	3.023	6.1
33R	3.003	2.9
15R	2.986	2.1

<sup>35</sup> To obtain phonon energies from absorption measurements alone, one must observe also the *phonon absorption* part of the spectrum, which requires measurements at higher temperatures.

<sup>36</sup> The energy gap usually quoted for semiconductors  $E_G$  is  $E_{Gx} + E_x$ , but the exciton binding energy  $E_x$  has not yet been measured for any SiC polytype.

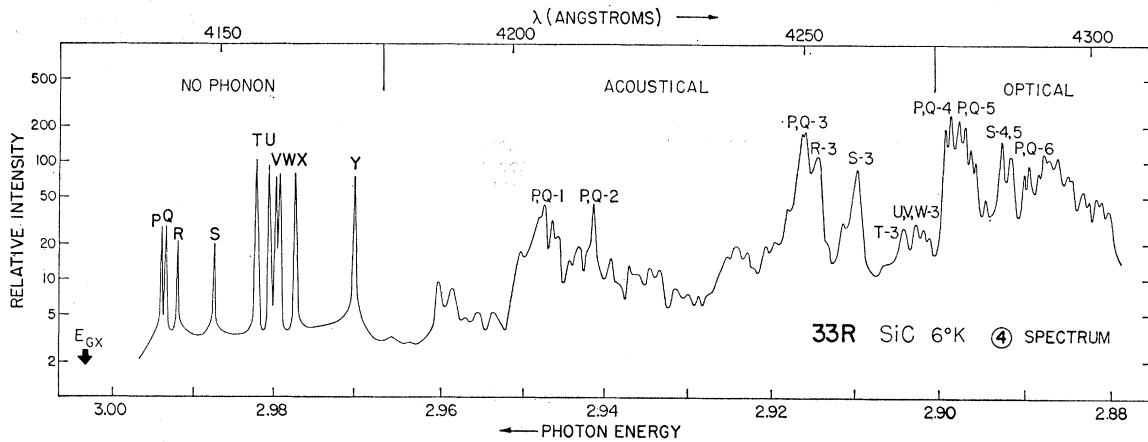


FIG. 3. Luminescence spectrum, at 6°K, of four-particle, nitrogen-exciton complexes in 33R SiC. Lines *P* to *Y* are ten no-phonon lines, due to complexes at ten of the eleven inequivalent nitrogen sites. Binding energies ( $E_{4x}$ ) at these sites are measured by the displacements of the lines from  $E_{Gx}$  (3.003 eV). Lines at the right are one-phonon lines, with the *P* and *Q* series most prominent. In this region, all marked lines involve one of the six "principal" phonons (numbered 1 to 6). Many weaker lines are due to emission of one of the other 60 phonons.

can be attributed to differences in conduction band minima.<sup>37</sup> The superposition of absorption edges suggests that we may be able to disregard differences in phonon interactions. We might then attribute the greater absorption strength of 6*H* to a greater density of states in the conduction band. The density of states is proportional to the number of minima (thought to be 12 for hexagonal polytypes and 6 for rhombohedral), and to the three-halves power of the electron effective mass. After dividing the 6*H* value of  $\alpha$  by two, to adjust for the number of valleys, there remains a slight indication that 6*H* has the largest electron effective mass, and 15*R* the smallest. The concept of a 33*R* electron mass intermediate between those of 6*H* and 15*R* proves to be very useful in interpreting the luminescence.

## VI. FOUR-PARTICLE SPECTRUM: EXPERIMENTAL RESULTS

In a semiconductor with indirect transitions, a *free* exciton can emit a photon only if a phonon is simultaneously emitted to conserve crystal momentum. A *bound* exciton, however, may, or may not, emit a phonon. No luminescence due to free excitons is observed in our samples. The 6°K photoluminescence spectrum shown in Fig. 3 is due to excitons bound to neutral donors at ten of the eleven inequivalent sites of 33*R* SiC. The ten lettered no-phonon lines, at the left in Fig. 3, are permitted *because* of the binding of the exciton, and the relative number of quanta in the no-phonon portion of the spectrum increases with increase of binding energy ( $E_{4x}$ ). Values of  $E_{4x}$  at the different sites are obtained by measuring the displacements in energy of the no-phonon lines from the exciton energy gap,  $E_{Gx}$  (3.003 eV).

<sup>37</sup> Reference 1, Sec. V.

Only ten no-phonon lines are observed, although nitrogen is almost certainly distributed over the eleven sites. In view of the intensity-binding relationship mentioned above, the missing line can scarcely be concealed in an unresolved doublet, hence it is thought to be missing because of a small value of  $E_{4x}$ . It was found in 6*H* SiC that complexes with small  $E_{4x}$  are unstable if the impurity density is high enough, apparently due to "exciton hopping" to the deeper levels.<sup>38</sup>

In the 15*R* photoluminescence spectrum, only four of the five inequivalent sites were observed. It will be shown that it is probably the "same" site which is responsible for the missing line in both 33*R* and 15*R* spectra.

We now turn to the phonon emission part of the spectrum. As there are 22 atoms per unit cell, we might have expected to see 66 lines for each of the no-phonon lines. The fact that the *strong* lines involve only a few phonons suggests the use of a large zone, which reduces the number of phonon branches to six. The six "principal" phonons are those with the same *k* value as the conduction band minima in the *large* zone.<sup>39</sup> They are easily recognized, because, in addition to giving rise to the strongest spectral lines, they have very nearly the same energies in all polytypes. The other ten phonons in each large zone branch are more weakly coupled, and most of them are not observed.

The spectrum is further simplified by the dominance of *P* and *Q* series, which are due to the two sites with smallest values of  $E_{4x}$ . Apparently, the donor sites with smallest  $E_{4x}$  have the largest capture cross sections for

<sup>38</sup> Reference 6, Sec. IV.

<sup>39</sup> In 6*H* SiC, where recombination radiation due to free excitons was observed, the *same* phonon energies were found in both intrinsic and four-particle spectra (Ref. 5, Sec. VI).

excitons, as observed also in other polytypes.<sup>40</sup> Thus, the spectrum is dominated by two of ten sites, and by six of 66 phonons.

The strongest lines in the phonon-emission portion of Fig. 3 are the six *P*, *Q* doublets, of which those marked 1 and 2 are TA, 3 is LA, 4 and 5 are TO, and 6 is LO.<sup>41</sup> The energies of these phonons are listed in Table IV and compared with those of 6*H* and 15*R*.<sup>42</sup> The close agreement indicates that the 33*R* conduction band minima are at the large zone boundary, as in 6*H* and 15*R*.

In Fig. 3, series other than *P* and *Q* are best seen for the LA phonon (No. 3), where the strong inverse intensity correlation with  $E_{4x}$  is observed. In the *P* and *Q* series, several lines due to phonons other than the "principal" phonons can be seen. Two of the most prominent unmarked lines correspond to phonon energies of 33.2 and 69.2 meV, which are close to energies of 6*H* and 15*R* phonons also. At the right, in the optical phonon region, many unmarked lines are not well resolved because the narrow range of optical phonon energies leads to a great deal of overlapping.

As one goes to higher polytypes of the series discussed in Sec. II, one expects the luminescence spectrum to approach that of 6*H*. This requires a similarity in phonon spectra which is already apparent in 33*R*. In Table IV, differences less than 0.3 meV are not significant, but where there are significant differences, as for the LA phonon, 33*R* is intermediate between 15*R* and 6*H*.

### VII. COMPARISON OF $E_{4x}$ VALUES IN THREE POLYTYPES

A comparison of 33*R* with 6*H* and 15*R* can now be made by using the accurately measured values of  $E_{4x}$ . The ten values obtained from Fig. 3 are plotted in

TABLE IV. Comparison of principal phonon energies in three polytypes. Energies in milli-electron volts. T=transverse, L=longitudinal; A=acoustic, O=optic.

Phonon number	Branch	6 <i>H</i>	33 <i>R</i>	15 <i>R</i>
1	TA <sub>1</sub>	46.3	46.3	46.3
2	TA <sub>2</sub>	53.5	52.3	51.9
3	LA	77.0	77.5	78.2
4	TO <sub>1</sub>	94.7	94.7	94.6
5	TO <sub>2</sub>	95.6	95.7	95.7
6	LO	104.2	103.7	103.7

<sup>40</sup> Reference 5, Sec. IVD.

<sup>41</sup> It is convenient, though not quite correct, to use the terminology transverse (T) and longitudinal (L), which we combine with acoustical (A) and optical (O).

<sup>42</sup> In the TO group, TO<sub>1</sub> is the phonon with smallest energy, and in 33*R*, the only other *strong* line is ascribed to TO<sub>2</sub>. For 6*H* and 15*R*, Table I of Ref. 7 does not identify TO<sub>1</sub> and TO<sub>2</sub>, but lists three TO phonons for 6*H*, and for 15*R*. We have taken the two *strongest* lines, in both 6*H* and 15*R*, to make the probable identification shown here. This is consistent with our observation that, in the acoustical branches, the large zone boundary, or "principal" phonons are the strongest.

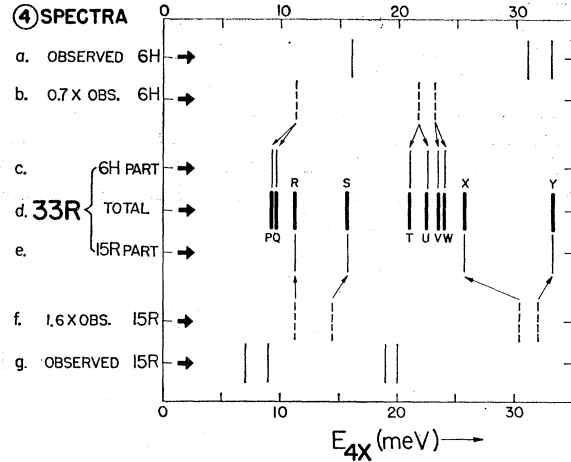


FIG. 4. Comparison of  $E_{4x}$  values in three polytypes. The observed values of  $E_{4x}$  for 33*R* (Row d) are separated into two parts, called 6*H* and 15*R* parts, in Rows c and e. The observed values of  $E_{4x}$  for 6*H* (Row a) are then adjusted empirically in Row b to correct for electron effective mass differences, and compared with the 6*H* part of 33*R*. A similar comparison is made for 15*R* in Rows e, f, and g.

Row d of Fig. 4. The proper separation of the ten lines into 6*H* and 15*R* parts, in Rows c and e, is most clearly demonstrated by using the code numbers derived in the following section. However, another way of making the separation is based on the expectation that the three 6*H* sites should give rise to three *pairs* of sites in 33*R*. Of all the no-phonon lines, *P*, *Q* and *V*, *W* are the two closest pairs, and, after they are taken out, *T* and *U* are the closest of those remaining. Hence, these three pairs are taken as the 6*H* part of 33*R*.

We now plot the experimental values<sup>43</sup> of  $E_{4x}$  for 6*H* and 15*R* in Rows a and g and consider what adjustments are necessary to compare these with the 6*H* and 15*R* parts of 33*R*. No calculations of  $E_{4x}$  values have been published, but there is an empirical proportionality to  $E_i$ , known as the Haynes rule,<sup>44,45</sup> and some limits for  $E_{4x}$  have been given, based on comparisons with hydrogen analogues.<sup>46</sup> There is certainly a dependence on hole and electron masses.<sup>31</sup> In SiC, we expect hole masses to be the same in the three polytypes, for the valence band maxima are at  $\mathbf{k}=0$ . However, electron masses will vary for the conduction band minima are at the large zone boundaries, which are different in the three polytypes.

If Haynes' rule and the effective mass approximation were valid for SiC donors, it would be easy to compare  $E_{4x}$  values for the "same" site in two polytypes. With  $E_{4x}$  proportional to  $E_c$ , and  $E_i$  proportional to the effective mass,<sup>47</sup> the  $E_{4x}$  ratios would be the same as the electron effective mass ratios. Because we have already

<sup>43</sup> Reference 7, Table II.

<sup>44</sup> J. R. Haynes, Phys. Rev. Letters 4, 361 (1960).

<sup>45</sup> R. E. Halsted and M. Aven, Phys. Rev. Letters 14, 64 (1965).

<sup>46</sup> W. Kohn, quoted in Ref. 44.

<sup>47</sup> W. Kohn, in *Solid State Physics*, edited by F. Seitz and D. Turnbull (Academic Press Inc., New York, 1957), Vol. 5, p. 257.

shown that we cannot use Haynes' rule for SiC,<sup>48</sup> and because we do not know the effective masses, we make an empirical "effective mass" correction. The  $6H$  values of  $E_{4x}$  in Row a are multiplied by 0.7 to obtain the values shown in Row b, which may then be compared with the  $6H$  part of  $33R$  in Row c. The only assumption needed here is that the same correction factor applies to all three inequivalent sites.

Applying the same procedure to the  $15R$  data, we find that multiplying the observed  $E_{4x}$  values by 1.6 gives energies which are close to those of the  $15R$  part of  $33R$ , with the exception of the  $X$  line, which is 20% off. The approximate fit of both  $6H$  and  $15R$  parts is evidence that there is some validity in the "effective mass" adjustments, and again suggests that the  $6H$  electron mass is the largest, the  $33R$  is intermediate, and the  $15R$  is the smallest, in agreement with the absorption data of Sec. V.

In comparing sites in the *same polytype*, however, something other than effective mass is required to explain donor ionization energy differences. Electron-spin resonance measurements,<sup>49</sup> for  $6H$  nitrogen donors, show equal hyperfine interaction at the three sites (within 1%), hence there is no appreciable central cell correction<sup>47</sup> to explain differences in  $E_i$ , or in  $E_{4x}$ . The observed differences have been attributed, instead, to the Kohn-Luttinger interference effect, which can pile up the electron density on a favorable (Si) or an unfavorable (C) sublattice.<sup>9</sup> Now, the positions of the conduction band minima may be similar in  $15R$  and  $33R$ , but they will not be exactly the same, and any differences will result in differences in the Kohn-Luttinger effects which, in turn, may account for the 20% disagreement for the  $X$  line.

It should also be noted that (a) the "same" site in two polytypes is the same out to a certain distance, but differs beyond that, and that (b) the ④ complex is a loosely bound complex. It will be shown that no disagreement comparable with that of the  $X$  line is observed for the tightly bound ③ complex.

### VIII. CODE FOR DONOR SITES

A compact description of inequivalent sites (a code) is necessary in order to compare different sites in the same polytype, or the "same" site in different polytypes. Fortunately, the required description is one-dimensional, as all differences depend only on the stacking order of equivalent planes. Thus, in the  $ABC$  notation, *planes* of atoms are described by single letters. This notation can be made more explicit by using capital letters for silicon planes, and small letters for carbon planes. The stacking order of  $6H$  SiC is shown in Fig. 5. If the Si-Si, or C-C interplanar distance of 2.52 Å is taken as four units (to avoid fractions), the distances

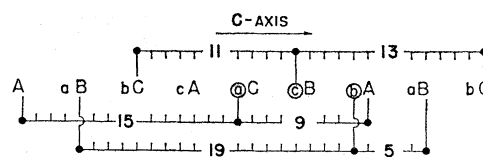


FIG. 5. Code numbers for the three inequivalent donors of  $6H$  SiC. The capital letters represent silicon planes, the small letters carbon planes. Nitrogen substitutes for carbon, as indicated by the circled letters. From each circled letter, the distances to "like" silicon planes are measured. These distances, in convenient units, constitute the numbers of the code, e.g., the  $a$  donor has the code 9, 15.

from a carbon plane to neighboring silicon planes are one and three units, a characteristic of tetrahedral bonding.

A simple code for a nitrogen donor site is obtained by giving the distances, in the above units, to "like" planes of *silicon* atoms. By "like" planes we mean planes represented by the same letter. For example, suppose a nitrogen donor to be substituted for carbon at the circled  $a$  in Fig. 5. Then the closest  $A$  plane is (as always) three units distant, but this superfluous number is omitted from the code. The next two  $A$  planes are 9 and 15 units distant, hence a simple code for this  $a$  site is 9, 15. By considering the next two more distant "like" planes, the code can be expanded to 9, 15, 21, 27. To keep the code as simple as possible, only enough terms need be retained to distinguish the sites unambiguously.

Various other codes could be used. We have chosen the code described above because of its simplicity, and for the following reasons. (a) For any site, the two kinds of "unlike" planes differ only in orientation, hence probably do not contribute much to site differences. The code is greatly simplified by omitting them. (b) The silicon sublattice is thought to be favored by the donor electron,<sup>50</sup> hence any reference to the carbon sublattice is omitted from the code.

Our code provides a simple method of *describing* the sites. To show that it can also be used for *ordering* the

TABLE V. Code numbers showing relationships between inequivalent sites of  $6H$ ,  $33R$ , and  $15R$ . The assignment of spectral lines to sites in  $33R$  is given at the left for the four-particle spectrum and at the right for the three-particle spectrum.

Lines in $33R$ ① spectrum	$6H$ sites	$33R$ sites	$15R$ sites	Line in $33R$ ② spectrum
...		13, 15, 21, 27	13, 15, 21, 29	$D$
$P$	11, 13, 21, 27	{ 11, 13, 21, 27		$B$
$Q$		{ 11, 13, 25, 27		$C$
$R$		{ 11, 13, 19, 21	11, 13, 19, 25	$A$
$S$		{ 9, 19, 21, 27	9, 19, 25, 27	$E$
$T$	9, 15, 21, 27	{ 9, 15, 21, 31		$F$
$U$		{ 9, 15, 25, 27		$G$
$V$	5, 19, 21, 27	{ 5, 19, 21, 27		$H$
$W$		{ 5, 19, 21, 29		( $H$ )
$X$		{ 5, 13, 19, 27	5, 13, 19, 29	$J$
$Y$		{ 5, 11, 21, 27	5, 11, 21, 27	...

<sup>48</sup> Reference 8, Sec. III.

<sup>49</sup> H. H. Woodbury and G. W. Ludwig, Phys. Rev. **124**, 1083 (1961).

<sup>50</sup> Reference 5, Sec. IX.

sites, for comparison with experiment, is the objective of the remainder of this section.

In Table V, we show the codes for all inequivalent sites in 6H, 33R, and 15R polytypes. Four code numbers are given so that all sites may be unambiguously distinguished. The separation of 33R sites into 6H and 15R parts is determined by the first code number in one instance, and by the second in all others, except for the 11,13 group where the third number is needed. A *difference* between a 33R site and the corresponding site of 6H or 15R (sometimes called the "same" site) is usually apparent in the third or fourth code number, although in three cases one must go beyond the fourth number. The first *different* number is italicized in the 33R column, the smallest such number being 21, which represents a distance of 13.2 Å. The *nearest* difference between corresponding sites is actually a difference in "unlike" planes at a distance of 17 units, or 10.7 Å (for two of the eleven sites).

A distance of 13.2 Å is thought to be greater than the effective Bohr radius in any of these polytypes.<sup>51</sup> Thus, the "same" site in two polytypes has neighborhoods so similar that binding-energy differences can probably be ascribed to differences in band properties, such as effective masses. Two 33R sites derived from a single 6H site, with similar neighborhoods and band properties, should therefore have *very* similar binding energies.<sup>52</sup>

The 33R code numbers in Table V are listed first in descending order of the first number, and then in descending order of the second. Those sites which have the same first and second numbers should give rise to nearby spectral lines. Thus, in the ④ spectrum, one expects the eleven no-phonon lines to fall into sets of 1,3,1,2,2,1, and 1. A correspondence with the observed ordering of  $E_{4x}$  is obtained in the way shown at the left of Table V. The missing line is assumed not to be bound because of a small  $E_{4x}$ . The second place is assigned to the *P* line (smallest *observed*  $E_{4x}$ ), and the others follow in order. Of the three lines *P*, *Q*, and *R* which are assigned to code 11,13, it is natural to consider the close pair *P*, *Q* as being derived from the single 6H line with code 11,13. The other close pair, *V*, *W*, is assigned automatically to the 5,19 line of 6H.

The discussion of Sec. VII shows that the above ordering is very satisfactory. On the other hand, it is easily seen that the reverse ordering would not work. The assignment of close pairs to 6H lines provides a critical test of any ordering scheme.

We cannot say why the chosen scheme works so well. It suggests that "like" planes are favored by the electrons of the complex. Such a conclusion was shown to be valid for 4H SiC donor electrons because of the Kohn-Luttinger interference effect,<sup>9</sup> but we should not extend that result to the polytypes being compared

<sup>51</sup> Using the free electron mass, and dielectric constant of 10.2, one obtains an effective Bohr radius of 5.4 Å.

<sup>52</sup> The extent to which binding energies are similar should also depend on the size of the complex.

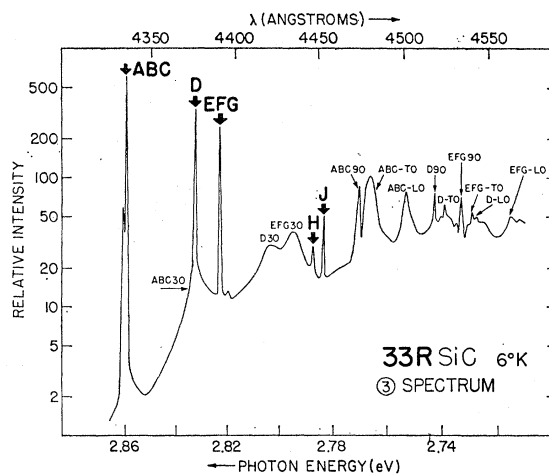


Fig. 6. A large portion of the three-particle spectrum at 6°K. No-phonon lines, some of which are unresolved here, are lettered A to J. Other lines are marked by series letter, and an identification of the emitted phonon.

here, as we do not know the positions of the conduction band minima.

### IX. THREE-PARTICLE SPECTRUM: EXPERIMENTAL RESULTS

At somewhat lower energies than those of the ④ spectrum, and not overlapping it, is another photoluminescence spectrum of quite different appearance. It is due to excitons bound to *ionized* nitrogen donors, at nine (perhaps ten) of the inequivalent sites in 33R SiC. Part of the spectrum at 6°K is shown in Fig. 6. This figure includes the no-phonon and a large part of the one-phonon spectrum. At lower energies still, off the right of Fig. 6, there are some broad two-phonon bands. Throughout the spectrum, many of the lines are strongly polarized.

The letters A to J indicate the no-phonon lines, some of which are so closely spaced as to be unresolved on this scale. With each no-phonon line is associated a series of lines due to phonon emission. However, for the tightly bound ③ complex, the phonons do not have the wave vector *k* of the conduction band minima. Instead, there is a broad band due to emission of an acoustic phonon, peaked at about 30 meV, and somewhat narrower bands identified as TO and LO. A sharper peak at 90 meV may be due to a localized phonon.

We shall not discuss this phonon spectrum, as it appears to be identical with that observed for 6H and 15R, and reported in Sec. VII of Ref. 7. Figure 6 of that reference shows a comparison of four-particle and three-particle phonon spectra for 15R.

To resolve the no-phonon groups ABC and EFG, we *immersed* the sample in liquid helium and reduced the temperature to 2°K by pumping. Figure 7 shows that the three peaks A, B, and C are of equal intensity, with B, and C barely resolved, the separation being about



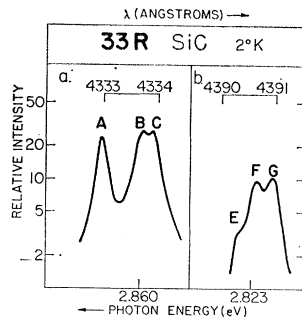


FIG. 7. Two groups of no-phonon lines at 2°K, and at high resolution. (a) The lines A, B, and C are of equal intensity, with total separation of 1 Å, or 0.6 meV. (b) The lines F and G are of equal intensity, as required for two lines corresponding to a single line of 6H.

0.1 meV. In the other group, F and G are of equal intensity, but E is much weaker.

### X. COMPARISON OF $E_{3z}$ VALUES IN THREE POLYTYPES

Another comparison of 33R with 6H and 15R can now be made, by using the accurately measured values of  $E_{3z}$ . The  $E_{3z}$  values are obtained from Figs. 6 and 7 by measuring the displacements in energy of the no-phonon lines from  $E_{G_x}$  (3.003eV), and they are plotted in Row d of Fig. 8. The line separations in the groups ABC and EFG have been exaggerated for clarity. The experimental  $E_{3z}$  values for 6H and 15R, obtained from Refs. 6 and 7, are plotted in Rows a and g.

We are following the scheme used for  $E_{4z}$  values in Sec. VII, and we can again look for pairs of lines to assign to the 6H part of the 33R spectrum in Row c. We take the close pair B,C, and, because they are not only close but of equal intensity, the pair F,G. It is clear that the size of the three-particle complex is such that the two 33R sites derived from each 6H site are nearly equivalent. No other pair of lines in Fig. 8 is close enough to be consistent with the B,C and F,G spacings, hence it is more likely that the third pair is unresolved.

If we now make "effective mass" adjustments of the 6H and 15R values, as shown in Rows b and f, we find that an excellent fit is obtained, provided the line H is taken as the unresolved doublet associated with the third 6H line. The polarization and the intensity ratios are also in agreement with this assignment. Most lines are polarized predominantly  $E||c$ , but the deeper levels are  $E\perp c$  (one in 6H, one in 15R, and two in 33R). The  $E\perp c$  lines are marked  $\perp$  in Fig. 8. The line intensities do not show any great regularity, but the third 6H line is very weak, and its relative strength is consistent with that of the line H of 33R, with which it is correlated.

By considering H to be an unresolved doublet, we have accounted for ten of the eleven inequivalent sites in 33R. The missing line in this spectrum is most likely to be that of a deep level, for a line can easily be lost among the phonon emission peaks at the right of Fig. 6. The same conclusion was drawn for the missing fifth line in the three-particle spectrum of 15R.

We now turn to the code in Table V. For most of the ③ no-phonon lines, the assignments follow the same

order used for the ④ spectrum, but the line D is a notable exception. The ABC lines are almost certainly due to the three sites with first two code numbers 11,13. The ③ complex is apparently small enough that the third code number is not very significant. We chose B and C as the pair corresponding to a 6H line, but any two of the ABC lines would be satisfactory, for they all have the same intensity. Thus, the order of the ABC lines in Table V is somewhat arbitrary.

The EFG lines are assigned to the three sites which have 9 as the first code number. One site has a different second code number, and, experimentally, one line has a quite different intensity. Thus, the separation in this group is clear. The missing lines of 15R and 33R are both assigned to the "same" site, with code 5,11. However, the order of 5,11 and 5,13 could be reversed.

Since we do not have a good explanation of the ordering, we cannot explain the failure of that order for the line D. The Kohn-Luttinger interference effects cannot be calculated, but they can be quite different for complexes of different size. For example, a favorable Si plane for a ④ complex may be beyond the significant distance for a ③ complex. In addition, the ④ complex has two electrons, the ③ complex only one. Thus the Kohn-Luttinger effects do not necessarily determine the same site ordering in the ④ and ③ spectra.

### XI. VALIDITY OF THE EFFECTIVE-MASS APPROXIMATION

Three different sets of experimental data have suggested that the 33R electron effective mass is intermediate between the large 6H mass and the smaller 15R mass. However, a comparison of Fig. 8 ( $E_{3z}$  values) with Fig. 4 ( $E_{4z}$  values) shows that much larger "effective mass" corrections were used in Fig. 4. The ratio of 6H to 15R masses suggested by these corrections is 2.28 in Fig. 4, but only 1.27 in Fig. 8. The ratio of 1.5, obtained from the absorption data, is rather speculative and poorly defined.

It was argued that the data fitting in Fig. 4 should give the true 6H to 15R mass ratio if SiC were a conventional semiconductor, defined as one in which Haynes' rule and the effective mass approximation are valid for shallow donors. It may also be argued that the data fitting in Fig. 8 should give almost the same ratio, in a conventional semiconductor, as  $E_{3z}$  is the principal part of  $E_i$  in Eq. (9). The fact that the ratio obtained from Fig. 8 is much smaller indicates that the ③ complex is more nearly the same in the three polytypes, i.e., more nearly independent of the band structure. In other words, it suggests that the effective mass approximation is not very good for the ③ complex. Whether or not the true effective mass ratio is near 2.28, as given by the ④ complex data, is an intriguing question. A cyclotron resonance measurement of the 6H and 15R masses is needed.

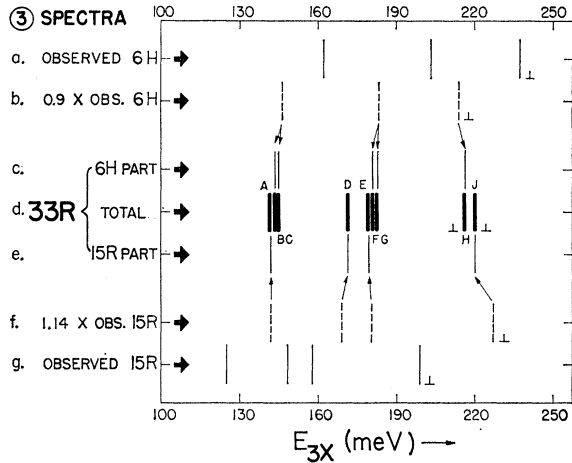


FIG. 8. Comparison of  $E_{3x}$  values in three polytypes. The observed values of  $E_{3x}$  for 33R (Row d) are separated into two parts, called 6H and 15R parts, in Rows c and e. The observed values of  $E_{3x}$  for 6H (Row a) are then adjusted empirically in Row b to correct for electron effective mass differences, and compared with the 6H part of 33R. A similar comparison is made for 15R in Rows e, f, and g. The separation of lines in the groups ABC and EFG has been exaggerated for clarity. In each row, the lines at the right are polarized  $E_{\perp c}$ , as indicated.

An important parameter in considering the validity of the effective mass approximation is the size of the complex. A pertinent observation is that the third code number is apparently important for the ④ complex, but not for the ③ complex. As an example, consider the two 9,15 sites, which differ in the third code number. The lines  $T$  and  $U$ , attributed to these sites in the ④ spectrum, are separated by 1.5 meV, or about 7% of  $E_{4x}$ . The lines  $F$  and  $G$ , however, attributed to the same sites in the ③ spectrum, are separated by only 0.2 meV, or about 0.1% of  $E_{3x}$ . The third code number for one of these sites is 21, which represents a distance of 13.2 Å.

If the effective-mass approximation is not valid for the ③ complex, the Kohn-Luttinger interference effect, which is based on this approximation, may also be reduced in importance. Thus, the Kohn-Luttinger effect may be responsible for the large range of  $E_{4x}$  values, but may not produce comparable differences in  $E_{3x}$  values. This would tend to invalidate Haynes' rule. Experimentally, the values of  $E_{4x}$  vary from 9 to 33 meV, nearly a factor of four. If Haynes' rule were valid, there would be a similar variation in  $E_i$ , instead of the observed variation of only 50% (see the following section).

## XII. NITROGEN-DONOR IONIZATION ENERGIES

The assignment of spectral lines to specific sites enables us to use Eq. (9) for the ionization energies, provided we can estimate  $E_4$ :

$$E_i = E_{3x} - E_{4x} + E_4. \quad (9)$$

An estimate of  $E_4$  involves  $E_x$  and  $E_3$  also. The way such estimates are made, and the experimental evidence used to justify them, are outlined for 6H donors in Sec. VI of Ref. 6. We follow the same procedure for 33R, but use a somewhat smaller effective mass, to obtain  $E_x \approx 50$  meV. For the complexes to which lines  $PQR$  and  $ABC$  are assigned, we estimate that  $E_4$  and  $E_3$  are about 20 and 40 meV, respectively. These values were used, with the appropriate  $E_{4x}$  and  $E_{3x}$ , in the energy level diagram of Sec. III (Fig. 1).

Since  $E_{4x}$  increases by 24 meV in going from  $P$  to  $Y$ , the sum of  $E_3$  and  $E_4$  must also increase by the same amount, as shown by Eq. (7). For this reason, we use values of  $E_4$  ranging from about 20 to 30 meV in Table VI. The estimated values of  $E_i$  then range from 0.15 to 0.23 eV. The comparable  $E_i$  values, estimated for 6H and 15R, are shown in Table II of Ref. 7. They range from 0.17 to 0.23 eV for 6H and 0.14 to 0.20 eV for 15R. As discussed above, the differences in electron effective masses may be somewhat larger than suggested by the differences in the ranges of ionization energies.

## XIII. THERMALLY EXCITED STATES OF THE COMPLEXES

In measurements at higher temperatures, additional spectral lines are observed in both ④ and ③ spectra. In the ④ spectrum, at about 20°K, only *one* additional line per site is seen. From it, a thermal excitation energy of 4.8 meV is obtained, independent of the site. The same excitation energy has been found in all polytypes studied, and is, therefore, independent of polytype also. Independence of site indicates that it is a *band* energy separation, and independence of polytype indicates that it is the *valence* band separation, i.e., the distance to the second of the three valence bands.<sup>58</sup> The third band, due to crystal-field splitting, has not been observed.

Our conclusion, that the second valence band is primarily due to the spin-orbit splitting, is based on the observation that the polarizations of the original and the extra lines appear to be the same.<sup>58</sup> However, the lines

TABLE VI. Nitrogen donor ionization energies, obtained by using Eq. (9) with measured values of exciton binding energies,  $E_{4x}$  and  $E_{3x}$ , and an estimated  $E_4$ . Energies in electron volts.

$E_{4x}$	$E_{3x}$	$E_{3x} - E_{4x}$	Estimated $E_i$
...	$D$ 0.171	<0.171	0.19
$P$ 0.0092	$B$ 0.143	0.134	0.15
$Q$ 0.0096	$C$ 0.143	0.133	0.15
$R$ 0.0112	$A$ 0.142	0.131	0.15
$S$ 0.0158	$E$ 0.180	0.164	0.18
$T$ 0.0210	$F$ 0.180	0.159	0.18
$U$ 0.0225	$G$ 0.180	0.158	0.18
$V$ 0.0234	$H$ 0.216	0.193	0.22
$W$ 0.0239	$H$ 0.216	0.192	0.22
$X$ 0.0257	$J$ 0.220	0.194	0.22
$Y$ 0.0332	...	>0.197	0.23

<sup>58</sup> The valence bands at  $\mathbf{k}=0$  are *qualitatively* like those of many materials with wurtzite structure. See Ref. 5, Sec. VB and Fig. 8.

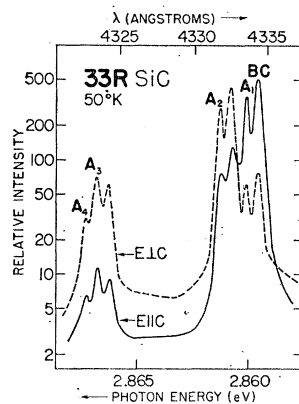


Fig. 9. A small part of the three-particle spectrum at 50°K. At low temperatures, only lines A, B, and C are observed, as shown in Fig. 7a. The additional lines are due to thermally excited states of the complexes, and they appear to be identical for all three sites (A, B, and C), including identical polarization. At this temperature, B and C are no longer resolved. The four A lines are marked,  $A_1$  being that due to the ground state [the A line of Fig. 7(a)]. There is good agreement between the observed intensity ratios and those given by a Boltzmann factor.

are rather weak for *good* polarization measurements, because, as the temperature is increased, the ④ spectrum vanishes before the thermally excited lines become very strong.

The measured 4.8 meV is interpreted as the band separation, but it is the true spin-orbit splitting only if the third band is sufficiently remote.<sup>54</sup> An upper limit for the spin-orbit energy of 8 meV was estimated in Ref. 53. Since the spin-orbit splitting is 6 meV in diamond,<sup>55</sup> and 44 meV in silicon,<sup>56</sup> even 8 meV is surprisingly small. However, Phillips<sup>57</sup> has shown that the interpretation of spin-orbit splitting is not straightforward in ionic crystals, and SiC has a fairly high degree of ionicity.<sup>58</sup>

The thermally excited lines of the ③ spectrum are of a different kind. The line separation from the fundamental varies from one site to another, and is, therefore, characteristic of the site and not of the band structure. This is consistent with previous indications that the ③ complex is small and tightly bound. For most of the sites, the thermally excited lines are obscured by other parts of the spectrum. For the *ABC* lines, however, a good spectrum is obtained at 50°K. Although lines *B* and *C* cannot be resolved at this temperature, it appears that three identical spectra are superimposed in Fig. 9.<sup>59</sup> These are due of course, to the three nearly identical sites with code 11,13.

In the *A* series, the fundamental line is marked  $A_1$ , and there are three thermally excited lines,  $A_2$ ,  $A_3$ , and  $A_4$ , with  $A_4$  about 7 meV higher than  $A_1$ . The

<sup>54</sup> For spin-orbit and crystal field interactions of the same order of magnitude, a calculation has been done by J. J. Hopfield, *J. Phys. Chem. Solids* **15**, 97 (1960).

<sup>55</sup> C. J. Rauch, in *Proceedings of the International Conference on the Physics of Semiconductors, Exeter, 1962* (The Institute of Physics and The Physical Society, London, 1962), p. 276.

<sup>56</sup> S. Zwerdling, K. J. Button, B. Lax, and L. M. Roth, *Phys. Rev. Letters* **4**, 173 (1960).

<sup>57</sup> J. C. Phillips, *Phys. Rev.* **136**, A1721 (1964).

<sup>58</sup> W. G. Spitzer, D. Kleinman, and D. Walsh, *Phys. Rev.* **113**, 127 (1959).

<sup>59</sup> In Figs. 3 and 6, we did not show the polarization of the luminescence because such information was not used. In Fig. 9, we show the polarization in order to emphasize the similarity of the *A*, *B*, and *C* spectra.

relative strengths are approximately given by the Boltzmann factor. At energies about 11 meV higher than  $A_4$ , there appears to be another line (or lines). Thus, there is a remarkable resemblance to the thermally excited spectrum shown<sup>60</sup> for *6H* and *15R* in Refs. 6 and 7. This is not so surprising when one realizes that the lines shown were the *A* lines in the *6H* and *15R* spectra, both of which are also assigned to the code 11,13 sites by Table V and Fig. 8. In other words, we have shown thermally excited states of the "same" site in three different polytypes, and these states depend more on the site than on the band structure. They appear to be nearly identical, even without an "effective-mass" correction, which is difficult to estimate for these broad lines.

In thermal stability, the ③ complexes are again intermediate between those of *6H* and *15R*, being more stable than those of *15R* (probably due to a larger value of  $E_g$ ), but less stable than those of *6H*. That is the reason we could not get a good spectrum at 77°K, as we did for *6H* in Ref. 6. Thus, the *33R* complexes probably have still higher excited states, like those reported for *6H*.

From a band structure point of view, the excited states might be attributed to a second valence band, and to valley-orbit splitting of the sixfold degenerate conduction-band minima. However, the evidence that the centers are small and tightly bound suggests that this point of view is inappropriate.

The doublets  $A_1, A_2$ , and  $A_3, A_4$  are rather suggestive of electron-hole *jj* coupling, which, for similar centers in GaP and ZnTe, gives rise to doublets in the luminescence spectra.<sup>61,62</sup> However, there is no indication that one line in each pair is forbidden, or even slightly forbidden, hence we think the doublets have a different origin in SiC.

#### XIV. HIGHER POLYTYPES

The *33R* photoluminescence spectrum has been interpreted by comparison with those of *6H* and *15R*, using properties of *bands*, and of *sites*. It should be possible to make such a comparison with *6H* and *15R* for any polytype in the series  $[(33)_n 32]_3$ , or, conversely, to make some predictions about the luminescence, given band and site properties.

The sites of any polytype in the series may be classified by means of our code, and the band properties may be assumed to approach those of *6H* for large *n*. The change in band properties is related to the changes in the large zone boundary and in the energy discontinuities,

<sup>60</sup> The line shown as  $A_3$  in the *6H* spectrum, in Fig. 7 of Ref. 6, was later split in a measurement at 50°K. Hence it corresponds to the pair  $A_3, A_4$  in the other polytypes. It may be noticed that the *6H* polarization, shown in this figure, is the same as that of *33R*.

<sup>61</sup> D. G. Thomas, M. Gershenzon, and J. J. Hopfield, *Phys. Rev.* **131**, 2397 (1963).

<sup>62</sup> R. E. Dietz, D. G. Thomas, and J. J. Hopfield, *Phys. Rev. Letters* **8**, 391 (1962).

as discussed in the following section. Presumably, the "effective mass" corrections, needed for the comparison of  $E_{4z}$  and  $E_{3z}$  values with those of  $6H$ , will steadily decrease with increasing  $n$ .

The site comparisons are straightforward. In higher polytypes of this series, the additional sites are of the  $6H$  variety, and, because the " $6H$ " portions increase, many of the sites are like those of  $6H$  to greater and greater distances. In  $51R$ ,  $[(33)_2 32]_3$ , for example, there are 17 inequivalent sites, with four sites corresponding to each one of  $6H$ . The resulting four lines will probably not be resolved in the  $\textcircled{3}$  spectrum. Hence the " $6H$  part" of  $51R$  will appear to generate three relatively strong lines. As  $n$  increases, these three lines will remain strong, each being generated by  $2n$  sites, and eventually they will coincide with the  $6H$  lines. Meanwhile, any one of the five " $15R$ " sites will give rise to a line that grows weaker as  $n$  increases, because it is generated by only one site in  $6n+5$ .

### XV. LARGE ZONES

Polytype comparisons in reciprocal space ( $\mathbf{k}$  space) are facilitated by the use of large zones.<sup>63</sup> An axial dimension of  $N\pi/c$  is chosen, where  $N$  is the number of close-packed layers in the stacking sequence (the number that appears in the Ramsdell symbol).  $N\pi/c$  is a constant, as the unit cell dimension  $c$  is proportional to  $N$ . The volume of the large zone is independent of polytype, and a considerable portion of it is free from strong energy discontinuities.

We show half a mirror plane of the  $33R$  large zone in Fig. 10, with a heavy line marking the zone boundary. Energy discontinuities within the zone are shown as light lines. These are of two kinds, broken horizontal lines, and solid oblique lines. The former represent extremely weak discontinuities, but the oblique lines represent significant discontinuities, and correspond to observable x-ray reflections. The only *horizontal* lines which represent strong discontinuities are the heavy top and bottom boundary lines, and these coincide for all polytypes.<sup>64</sup> The boundary lines that *change* with polytype are those that form the right boundary, of which the largest parts correspond to the  $(10\bar{1},16)$  and  $(10\bar{1},17)$  reflections in  $33R$ .<sup>65</sup>

We again consider the polytype series with Zhdanov symbol  $[(33)_n 32]_3$ , of which  $33R$  is the member with  $n=1$ . These rhombohedral polytypes approach the hexagonal  $6H$  for large  $n$ , or large  $N$  in the Ramsdell symbol  $NR$ , with  $N=18n+15$  (see Table I). By looking at Fig. 10 for  $33R$ , we can visualize the further changes necessary to transform this mirror plane into a mirror plane of the  $6H$  large zone.

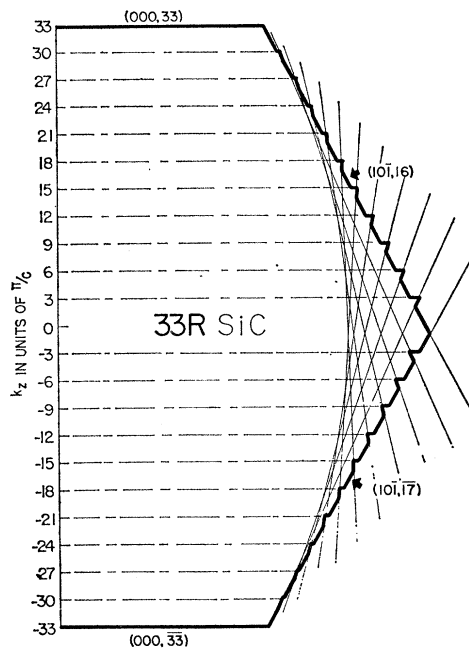


FIG. 10. Half a mirror plane of a large zone for  $33R$  SiC. The heavy line is the zone boundary. Lighter lines represent energy discontinuities, of which there are two kinds. Those corresponding to the broken horizontal lines are extremely weak, hence most of the large zone is free of strong discontinuities. The rest of the zone, at the right, is cut by a network of energy discontinuities (the oblique lines), some of which are strong. The conduction-band minima are thought to be on the right boundary, where the significant changes occur, with changing polytype.

The top and bottom ( $t$  and  $b$ ) right boundary planes<sup>66</sup> for a general rhombohedral polytype,  $NR$ , correspond to the x-ray reflections  $(10\bar{1},t)$  and  $(10\bar{1},b)$ , with  $t=\frac{1}{2}(n-1)$ , and  $b=\frac{1}{2}(n+1)$ . For cubic, considered as  $3R$ ,  $t$  and  $b$  are 1 and 2, which, in cubic notation, correspond to the  $(1\bar{1}1)$  and  $(0\bar{2}0)$  reflections, i.e., to the hexagonal and square faces of the cubic Brillouin zone.<sup>67</sup> For  $33R$ ,  $t$  and  $b$  are 16 and 17, and, as  $N$  increases,  $t$  and  $b$  both approach  $N/2$  asymptotically, and the reflections then become equivalent to the corresponding  $6H$  reflections.

The dentations in the boundary become more numerous, but smaller, as  $N$  increases, soon becoming only a small ripple in the boundary, and finally vanishing asymptotically. The energy discontinuities within the large zone also become more numerous with increasing  $N$ , but the x-ray work shows that only those corresponding to  $6H$  discontinuities remain strong, the others being negligible for large  $N$ .<sup>26</sup>

The boundaries of  $33R$  and  $6H$  are already so close that the  $6H$  boundary could not be shown clearly in Fig.

<sup>66</sup> We refer to the principal boundary planes, excluding the dentations.

<sup>67</sup> Relationships to other rhombohedral polytypes are clarified by considering cubic as the fundamental rhombohedral polytype  $3R$ , and by using the Bravais-Miller notation. The cubic  $(1011)$  and  $(101\bar{2})$  reflections coincide with the  $(10\bar{1},11)$  and  $(10\bar{1},22)$  reflections of  $33R$ . See also Fig. 4 of Ref. 8.

<sup>63</sup> The large zone for  $4H$  polytype is discussed in Ref. 1, and that for  $21R$  in Ref. 8.

<sup>64</sup> In general, these are the  $(000, \pm N)$  reflections. See, for example, F. G. Smith, *Am. Mineralogist* **40**, 658 (1955).

<sup>65</sup> Energy discontinuities are labeled by the Bravais-Miller indices of the corresponding x-ray reflections.

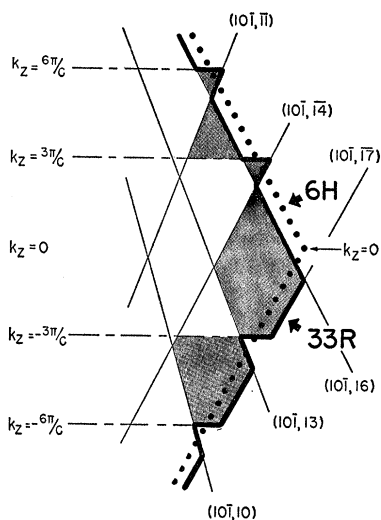


FIG. 11. A comparison of  $33R$  and  $6H$  large zones. A portion of the  $33R$  mirror plane of Fig. 10 is shown here on a larger scale, so that the rather small differences between  $33R$  and  $6H$  zones can be seen. The dotted  $6H$  boundary cuts the indentations of the  $33R$  boundary, thus going in and out of the  $33R$  boundary many times.

10. The greatest difference between the two occurs at the right corner (near  $k_z=0$ ). An enlarged drawing of this region is shown in Fig. 11, with the  $6H$  boundary indicated by the dotted line.<sup>68</sup>

We have conjectured that, in *all* polytypes, the conduction band minima are on mirror planes, and at the large zone boundary<sup>1</sup> (on the right boundary, in Fig. 10, for  $33R$ , and at the corresponding boundary in other polytypes). We assume that the interior of the zone is changed very little by polytype changes, and that the observed changes in exciton energy gaps, and in electron effective masses are results of the changing right boundary, and the changing network of energy discontinuities near it.

The way in which the six conduction band minima<sup>69</sup> in rhombohedral polytypes become twelve in  $6H$  is also

<sup>68</sup> The complete large zone can be reduced to eleven Brillouin zones, and portions of the eleventh zone form the boundary of the large zone. Several of these portions are shaded in Fig. 11.

<sup>69</sup> For  $33R$ , there is one position, on the boundary at  $k_z = -17\pi/c$ , which could give only *three* minima, but there does not appear to be any good reason to favor this position.

of interest. If  $33R$  has six minima in positions equivalent by symmetry to one on the *bottom* right boundary, then there will be another set of six *higher* minima (secondary minima) in positions equivalent by symmetry to one on the *top* right boundary. These two sets must approach each other in the higher polytypes of the  $[(33)_n 32]_3$  series, eventually forming the set of twelve minima for  $6H$ .

The six secondary minima in  $33R$  are not observed. They could contribute to thermally excited states of the complexes, but we saw no lines, in the luminescence measurements at higher temperatures, which were not also seen in the  $6H$  spectrum.

## XVI. PRINCIPAL CONCLUSIONS

Absorption and luminescence measurements on  $33R$  SiC yield a variety of band and site parameters. However, the principal conclusions are based on a comparison of  $33R$  with  $6H$  and  $15R$ , the two polytypes which, in a sense, constitute the  $33R$  structural units. The validity of this point of view is clarified by the use of a code which assigns each of the eleven donor sites in  $33R$  to a " $6H$  part" or a " $15$  part."

Among the unusual comparisons made possible by this procedure is that of  $6H$  and  $15R$  electron effective masses (Sec. XI). Previous measurements, on  $6H$  and  $15R$  polytypes themselves, suggested that the  $15R$  mass was smaller, but a *numerical* value of mass ratios is obtained only by an interpretation which recognizes the " $6H$  and  $15R$  parts" in the  $33R$  spectra. There is a conflict between effective mass ratios obtained from four-particle and from three-particle spectra. This is pertinent to a discussion of the validity of the effective-mass approximation for nitrogen donors in SiC.

The procedure used for  $33R$  can also be applied to  $51R$ , and to a certain series of higher polytypes. We can predict some properties of the luminescence of these higher polytypes, and we use a large zone to show how their band properties approach those of  $6H$  asymptotically.

## ACKNOWLEDGMENT

We wish to thank M. M. Sopira, Jr., for technical assistance.